Proceedings of the 1999 IEEE
International Conference on Robotics & Automation
Detroit, Michigan • May 1999

Design of a Spider-Like Robot for Motion with Quasistatic Force Constraints

Shraga Shoval
IE Department, Technion
shraga@hitech.technion.ac.il

Elon Rimon
ME Department, Technion
elon@robby.technion.ac.il

Amir Shapiro
ME Department, Technion
amirs@tx.technion.ac.il

Abstract: *This paper presents a novel design of a 4-legged "spider" robot capable of moving in a wide range of two-dimensional tunnels. The spider moves in a quasistatic manner, by stably bracing itself against the tunnel walls and moving a free limb to a new position. The design has been strongly influenced by the recent immobilization theory of Rimon and Burdick [13, 15]. The theory dictates the minimum number of limbs such a spider can have, as well as the shape of the footpads. The class of tunnel geometries dictates other key parameters of the spider, such as limb dimensions and number of degrees of freedom of each limb. We review the relevant components of the immobilization theory, then describe the details of the spider design. The spider will initially move under a worst-case assumption of slippery tunnel walls, and we also describe a locomotion strategy under this assumption. The spider has been built and is currently undergoing locomotion experiments.*

1 Introduction

Many motion planning problems are suited for legged robots that interact with the environment in order to achieve stable locomotion. For example, surveillance of collapsed structures for survivors, inspection and testing of aircraft engine and wing interiors, and inspection of hazardous structures such as nuclear reactors, all require motion in a congested, unstructured, and complex environment. Further, in such environments the robot cannot always rely on friction, as surfaces may be wet, oily, or icy. Our goal is to develop a general purpose multi-legged mechanism that uses quasistatic motion to navigate in such environments. In *quasistatic motion*, inertial effects due to moving parts are kept small relative to the forces/torques of interaction between the robot and the environment. Motion is generated by reaction forces between the robot and the environment, and the planning of a path to the goal is subject to the constraint of maintaining stable equilibrium with the environment during the motion. Spider-like and snake-like mechanisms are examples of robots that can move quasistatically in congested environments. We now mention several works in these two areas.

In prior work on spider-like mechanisms, the robot typically moves according to a set of heuristically chosen locomotion modes, or by simple local reactive control laws. While these types of motion guarantee stable behavior of each individual limb, they do not necessarily guarantee stability of the whole mechanism. Examples of such spider-like mechanisms are by Madhani and Dubowsky [6], Neubauer [10], and Stone et. al. [17]. Legged locomotion in a gravitational field is related to locomotion in congested environments. Examples of works in this area are by Boissonnat [1], Hirose [4], Marhefka [7], McGeer [9], Pfeiffer [11], Van-den-Doel [18], and their coworkers. However, we focus on locomotion in congested tunnel-like environments rather than legged locomotion over a terrain.

Snake-like mechanisms also interact with the environment during locomotion. They are related to spider-like mechanisms, since both mechanisms brace themselves against the environment while moving free parts toward a new position. Chrikjian and Burdick [2] and Shan and Koren [16] developed snake-like mechanisms that move by locking some of their links to the ground while allowing other links to move. These workers, as well as Hirose and Morishima [5], also investigated the use of motion patterns borrowed from biological snakes. However, virtually all existing snake-like mechanisms interact with the environment via frictional contacts with the ground. In contrast, we focus on locomotion where the robot stably braces itself against the environment while moving its free parts. Furthermore, our robot is required to operate under the worst-case assumption of slippery contacts.

Our goal is thus to design a spider-like mechanism that can move in congested unstructured environments. We make the following assumptions. First, we initially study locomotion in *two-dimensional horizontal tunnels with piecewise linear walls*. Second, we assume that the tunnel has *slippery walls*, so that locomotion must proceed without using friction. This restriction excludes tunnels of a particular simple geometry (such as two parallel lines), but most unstructured congested environments do have a complex geometry with many possible

0-7803-5180-0-5/99 $10.00 © 1999 IEEE

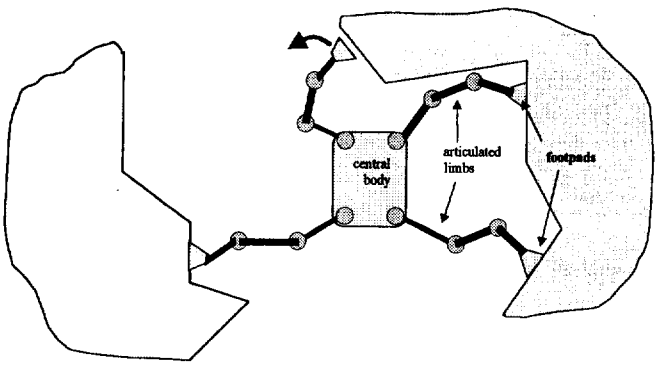

Figure 1. A conceptual design of a spider-like robot moving in a two-dimensional tunnel.

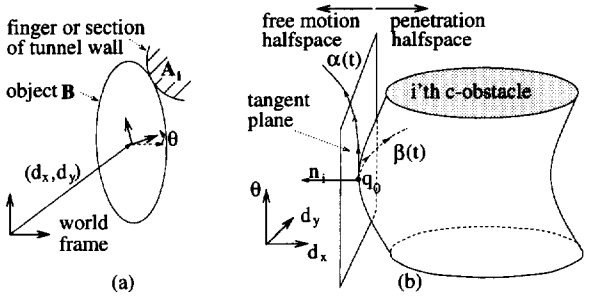

Figure 2. The first-order approximation to the free motions of $\mathcal{B}$ at q_0. $\dot{\alpha}(0)$ and $\dot{\beta}(0)$ are 1^{st} order roll-slide motions. $\alpha(t)$ locally lies in freespace, $\beta(t)$ locally penetrates the c-obstacle.

footholds within reach of the robot. Our last assumption is that the spider moves quasistatically, by stably bracing itself against the tunnel walls while changing its internal configuration to allow motion of its free parts to the next position. This approach enables the robot to reliably operate even when unpredicted external forces are applied, such as drag forces from surrounding air or liquids, unexpected collisions, or uneven loads.

We describe the design of a 4-legged spider robot (Figure 1), capable of quasistatically moving in a wide range of two-dimensional tunnels according to the above assumptions. The design has been strongly influenced by the recent immobilization theory of Rimon and Burdick [13, 15]. The theory dictates the minimum number of limbs such a spider can have, as well as the shape of the footpads. The class of tunnel geometries dictates other key parameters of the spider, such as limb dimensions and number of degrees of freedom of each limb. We begin with a review of the immobilization theory and its implications for the spider's structure. Then we describe the spider design, accounting for issues such as the number of degrees-of-freedom of each limb, links dimension, and the mechanical structure of various parts of the spider. The spider will initially move under a worst-case assumption of slippery tunnel walls, and we also describe a locomotion strategy under this assumption. The spider has been built and is currently undergoing locomotion experiments in a tunnel.

2 C-Space Approach to Rigid Body Mobility

The immobilization theory developed by Rimon and Burdick [13, 15] provides a basis for the design of the spider robot. This theory is concerned with the mobility of a rigid object $\mathcal{B}$ held by k stationary and *frictionless* finger bodies $\mathcal{A}_1, \ldots, \mathcal{A}_k$ in an equilibrium grasp. The same analysis holds for a k-limb mechanism which braces itself against an environment in a static equilibrium posture. In the latter case the mechanism plays the role of $\mathcal{B}$, while the tunnel walls play the role of $\mathcal{A}_1, \ldots, \mathcal{A}_k$. The bodies are planar, and the analysis focuses on the configuration space (*c-space*) of $\mathcal{B}$, parametrized by $q = (d_x, d_y, \theta) \in I\!R^3$. The fingers or tunnel walls are represented as c-space obstacles (*c-obstacles*). As shown in Figure 2, the c-obstacle due to $\mathcal{A}_i$ is the set of all configurations where $\mathcal{B}$ intersects the stationary $\mathcal{A}_i$. Thus, if q_0 is $\mathcal{B}$'s contact configuration with $\mathcal{A}_i$, q_0 lies on the c-obstacle boundary, denoted $\mathcal{S}_i$. When $\mathcal{B}$ is contacted by k bodies, q_0 lies on the intersection of $\mathcal{S}_i$ for $i = 1, ..., k$. We denote tangent vectors in c-space by $\dot{q}$, and use the notation $T_q I\!R^3$ and $T_q \mathcal{S}_i$ for the tangent space of $I\!R^3$ and $\mathcal{S}_i$ at q.

2.1 1^{st} and 2^{nd} order free motions

The *free motions* of $\mathcal{B}$ are those local motions of $\mathcal{B}$ along which it either breaks away from or maintains surface contact with the bodies $\mathcal{A}_1, \ldots, \mathcal{A}_k$. In c-space, the free motions of $\mathcal{B}$ at q_0 are the c-space paths that emanate from q_0 and locally lie in the *freespace*, which is the complement of the c-obstacle interiors. The first-order geometry of the free paths and the c-obstacle boundaries determines what we term the *first-order mobility* of $\mathcal{B}$ at q_0. To formalize this notion, let $\mathrm{n}_i(q_0)$ be the outward pointing unit normal to $\mathcal{S}_i$ at q_0 (Fig. 2(b)). The 1^{st} *order free motions* of $\mathcal{B}$ at q_0 is the halfspace of tangent vectors $\dot{q} \in T_{q_0} I\!R^3$ satisfying $M_i^1(q_0) \triangleq \{\dot{q} \in T_{q_0} I\!R^3 : \mathrm{n}_i(q_0) \cdot \dot{q} \geq 0\}$. Tangent vectors $\dot{q} \in T_{q_0} I\!R^3$ satisfying $\mathrm{n}_i(q_0) \cdot \dot{q} = 0$ are called 1^{st} *order roll-slide motions*, while the other tangent vectors in $M_i^1(q_0)$ are called 1^{st} *order escape motions*. For k fingers or tunnel walls, the set of 1^{st} order free motions is: $M_{1,\ldots,k}^1(q_0) \triangleq \cap_{i=1}^k M_i^1(q_0)$.

Thus, along 1^{st} order escape motions $\mathcal{B}$ locally breaks away from $\mathcal{A}_i$. Along 1^{st} order roll-slide motions $\mathcal{B}$ maintains surface contact with $\mathcal{A}_i$ to first-order, and *it is not possible* to determine from first-order considerations if $\mathcal{B}$ locally breaks away or penetrates $\mathcal{A}_i$. For example, the c-space curves $\alpha(t)$ and $\beta(t)$ in Figure 2 have the same tangent vector at q_0. Yet $\alpha(t)$ locally lies

in the freespace, while $\beta(t)$ does not. As we shall see, *all the free motions of $\mathcal{B}$ at a frictionless equilibrium grasp or posture are necessarily roll-slide to first-order.* Thus, in order to fully characterize the mobility of $\mathcal{B}$, the second-order properties of its local motions must be considered. The ensuing characterization of second-order mobility is a major new tool which we employ in the design of the spider robot.

The second-order geometry of the free-motion curves and the c-obstacles is determined by their curvature and curvature form, respectively. The *curvature form*, describing the curvature of $\mathcal{S}_i$ at $q_0 \in \mathcal{S}_i$, is the quadratic form $\kappa_i(q_0, \dot{q}) \triangleq \dot{q}^T Dn_i(q_0)\dot{q}$, where $\dot{q} \in T_{q_0}\mathcal{S}_i$ and Dn_i is the derivative of the unit normal n_i. Ref. [13] contains a formula for $\kappa_i(q_0, \dot{q})$ in terms of the surface normals and curvatures of the contacting bodies. The free-motion curves are determined to second-order by their *velocity and acceleration* at q_0, as follows. The 2^{nd} *order free motions* of $\mathcal{B}$ at q_0 is the subset of $(\dot{q}, \ddot{q})$ satisfying $M_i^2(q_0) \triangleq \{(\dot{q}, \ddot{q}) : \mathrm{n}_i(q_0) \cdot \dot{q} = 0$ and $\dot{q}^T[Dn_i(q_0)]\dot{q} + \mathrm{n}_i(q_0) \cdot \ddot{q} \geq 0\}$. Analogous to the first-order case, pairs $(\dot{q}, \ddot{q})$ that satisfy $\mathrm{n}_i(q_0) \cdot \dot{q} = 0$ and $\dot{q}^T[Dn_i(q_0)]\dot{q} + \mathrm{n}_i(q_0) \cdot \ddot{q} = 0$ are called 2^{nd} *order roll-slide motions*, while the other pairs in $M_i^2(q_0)$ are called 2^{nd} *order escape motions.* Note that the definition of 2^{nd} order free motions focuses on those curves which are 1^{st} order roll-slide motions, but might not correspond to free-motion curves. It is important to stress that 1^{st} order roll-slide motions are the only motions available for $\mathcal{B}$ when it is held in an equilibrium grasp or posture. Thus, if all the 1^{st} order roll-slide motions of $\mathcal{B}$ are 2^{nd} order penetration motions, $\mathcal{B}$ is completely immobilized at the equilibrium.

2.2 1^{st} and 2^{nd} Order Mobility Indices

We now use the free-motion framework to define *mobility indices.* These are coordinate invariant integer-valued functions that measure the instantaneous mobility of $\mathcal{B}$ when it is held in a k-contact equilibrium grasp or posture. At an equilibrium the net wrench (force and torque) generated by the contact forces is zero. It can be verified that the wrench generated by the i^{th} contact force is a positive multiple of the c-obstacle normal $\mathrm{n}_i(q_0)$. An *equilibrium grasp* is therefore characterized by the condition that zero lies in the convex hull of $\mathrm{n}_1(q_0), ..., \mathrm{n}_k(q_0)$. That is, there exist scalars $\lambda_1, ..., \lambda_k$ such that

$$\vec{0} = \lambda_1 \mathrm{n}_1(q_0) + \cdots + \lambda_k \mathrm{n}_k(q_0), \qquad (1)$$

where $\lambda_i \geq 0$ and $\sum_{i=1}^k \lambda_i = 1$.

At a k-contact equilibrium grasp/posture, the intersection of the 1^{st} order free motion halfspaces associated with the individual contacts forms a subspace. This subspace is the set of instantaneous motions which are simultaneously 1^{st} order free with respect to each of the bodies $\mathcal{A}_1, \ldots, \mathcal{A}_k$. The 1^{st} *order mobility index* of an equilibrium grasp/posture is defined as the dimension of this subspace. The index is denoted $m^1_{q_0}$, and for non-redundant grasps $m^1_{q_0} = \max\{0, 4-k\}$ where k is the number of contacts. A key fact is that $m^1_{q_0}$ *is identical for all k-contact equilibrium grasps or postures.*

The 2^{nd} order mobility index for k-contact equilibrium grasps/postures is based on the c-space curvature form of $\mathcal{S}_i$, $\kappa_i(q_0, \dot{q})$. Consider the coefficients λ_i in the equilibrium condition (1). It is shown in [15] that the weighted sum of the c-obstacle curvatures, called the *relative c-space curvature*, has a coordinate invariant structure which is related to the second-order mobility of $\mathcal{B}$ at the equilibrium. These notions are made precise in the following definition.

Definition 1 *Let $\lambda_1, ..., \lambda_k$ be the coefficients of the equilibrium equation* (1). *The* **c-space relative curvature form** *for the equilibrium is the quadratic form:*

$$\kappa_{\mathrm{rel}}(q_0, \dot{q}) = \sum_{i=1}^{k} \lambda_i \kappa_i(q_0, \dot{q}) \quad \textit{such that } \dot{q} \in M^1_{1,\ldots,k}(q_0).$$

The **2^{nd} order mobility index** *of the equilibrium, denoted $m^2_{q_0}$, is the* **number of non-negative eigenvalues** *of the matrix of the c-space relative curvature $\kappa_{\mathrm{rel}}(q_0, \dot{q})$.*

By definition, $m^1_{q_0}$ is an upper bound on the possible values of $m^2_{q_0}$ i.e., $0 \leq m^2_{q_0} \leq m^1_{q_0}$. Hence *second-order (or curvature) effects always act to reduce the mobility of $\mathcal{B}$.* We say that $\mathcal{B}$ is *completely immobile* if its configuration q_0 is completely isolated from the freespace by the c-obstacles associated with the bodies $\mathcal{A}_1, \ldots, \mathcal{A}_k$. Physically, this means that all the local c-space motions of $\mathcal{B}$ which start at q_0 cause the object to penetrate the bodies $\mathcal{A}_1, \ldots, \mathcal{A}_k$. We say that $\mathcal{B}$ is *immobile to first-order* if $m^1_{q_0} = 0$, and *immobile to second-order* if $m^2_{q_0} = 0$. For $k \geq 4$ contacts $m^1_{q_0} = 0$, and $\mathcal{B}$ is completely immobile to first-order. The 2^{nd} order index is useful for determining the mobility of $\mathcal{B}$ in planar grasps or postures involving $k = 2, 3$ contacts. In these cases $\mathcal{B}$ is not immobile to first-order ($m^1_{q_0} > 0$), but may be immobile to second-order ($m^2_{q_0} = 0$).

2.3 Implications for the Spider's Design

Here we briefly sketch some implications of the immobilization theory to the spider's structure. The 1^{st} and 2^{nd} order mobility indices allow immobilization which is based on surface curvature in addition to the more conventional reliance on contact normals. Based on conventional first-order considerations, it was previously thought that *four* frictionless contacts are required to immobilize generic 2D objects [8, 12]. However, Czyzowicz et. al. [3] and Rimon and Burdick [14] have shown that generic 2D objects can be immobilized by

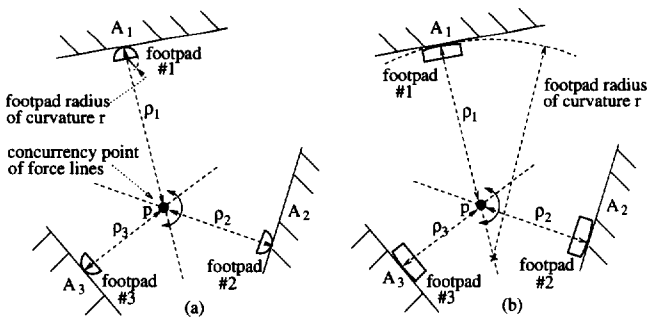

Figure 3. (a) The spider is not immobile since $r < \rho_i$. (b) The spider is immobile since the footpads satisfy $r > \rho_i$.

only *three* frictionless fingers with convex boundary, provided that the fingers are sufficiently flat at the contacts. Equivalently, *any multi-limbed mechanism can immobilize itself against a frictionless environment using only three limbs with sufficiently flat convex footpads.* The spider must therefore have at least *four* limbs—three for immobilization and at least one additional limb for establishing a new foothold during locomotion.

Let us consider the proper choice of footpad curvature. In a 3-legged equilibrium posture, the contact-force lines must intersect at a common point p (Fig. 3). The set of 1^{st} order roll-slide motions available to the mechanism is a one-dimensional subspace (since $m^1_{q_0} = 1$), consisting of instantaneous rotations of the mechanism about p. (That is, instantaneous rotations of the mechanism as a single rigid body.) For complete immobility we must have $m^2_{q_0} = 0$. This condition can be interpreted as the requirement that the footpads be sufficiently flat at the contacts, as to prevent instantaneous rotations of the mechanism about p. A sufficient condition for $m^2_{q_0} = 0$ is that *the radius of curvature of the i^{th} footpad be larger than the distance between the i^{th} contact point and the concurrency point p, for $i = 1, 2, 3$.* This condition is illustrated in Figure 3, where the footpads have a radius of curvature r, and the distance between the i^{th} contact and p is denoted ρ_i. In our design, we have selected the footpads' radius-of-curvature to be slightly larger than the tunnel's average width, thereby guaranteeing that the mechanism will be completely immobile in every 3-legged equilibrium posture.

3 Spider Robot Design Considerations

Thus far we have established that the spider will have four limbs, with the footpads' curvature sufficiently flat as to guarantee immobilization. In this section we describe the considerations that have led us to choose other key parameters of the spider. First we consider kinematic parameters—the number of degrees of freedom and the links' dimension. Then we consider the mechanical structure of the spider's limbs and footpads.

3.1 The Number of Degrees of Freedom

As discussed below, the spider uses two modes of locomotion. In the first mode, called *limb repositioning*, the spider braces itself against the environment with three limbs and lifts its fourth limb to a new position. In the second mode, called *central-body repositioning*, the spider contacts the environment with all four limbs while repositioning its central body at a new location.

We now discuss our choice of the number of degrees of freedom (d.o.f.) for each limb. First consider the central-body repositioning mode of locomotion. To allow arbitrary placement of the central body in the plane (position and orientation), the closed-loop mechanism formed by the spider should have at least three d.o.f.. In general, the number of d.o.f. of a planar mechanism consisting of #link links and #joint joints is:

$$\#\,\text{d.o.f.} = 3(\#\text{link} - 1_{\text{environment}}) - 2\#\text{joint}, \qquad (2)$$

where #link includes a stationary link representing the environment. Let n be the number of links in each limb. There are n joints in each limb, and consequently $\#\text{joint} = 4n$. The spider has four limbs, and the distal link of each limb (the footpad) remains stationary. Hence $\#\text{link} = 4n + 1_{\text{central-body}} + 1_{\text{environment}} - 4_{\text{footpads}}$. Substituting these values in (2) gives:

$$\begin{aligned} \#\ \text{d.o.f.} &= 3(4n + 1_{\text{central-body}} - 4_{\text{footpads}}) \\ &\quad -8n = 4n - 9. \end{aligned}$$

The requirement $\#\,\text{d.o.f.} = 4n - 9 \geq 3$ implies that $n \geq 3$. Thus *three* links and *three* joints for each limb would suffice during central-body repositioning. Consider now the limb-repositioning mode of locomotion. We may assume that the central-body makes only local motions during this mode of locomotion. The free limb therefore has an essentially fixed base while it attempts to reach a new foothold position. In principal the limb's three d.o.f. should suffice to arbitrarily place its footpad in the plane (position and orientation). However, when operating in a congested environment, additional d.o.f. are required in order to accommodate obstacles. But motion planning and control become substantially more complex as the number of d.o.f. increases. Thus, in order to increase maneuverability while retaining a manageable mechanism complexity, we add *one* additional link and joint to each limb, resulting in *four* links and *four* joints for each limb.

3.2 The Spider's Dimensions

We now describe our choice of two key dimensions of the spider robot: the size of the central-body, denoted b, and the total length of each limb, denoted l. (The dimension of the individual links is determined below.) The ratio l/b is related to the desired maneuverability of

the spider as follows. Let D_{min} and D_{max} be the minimal and maximal widths of the tunnel. Then $D_{min} \geq b$ to allow motion of the central body through the tunnel, while $D_{max} \leq b + 2l$ to allow the spider to reach both sides of the tunnel. Assuming that $D_{min} = b$ and $D_{max} = b + 2l$, we define the *maneuverability index* as the ratio: $M = D_{max}/D_{min} = 1 + 2l/b$. A large maneuverability index is more desirable, as it reflects an increased ability of the spider to move in a given tunnel environment. In our design, we have assumed tunnels with a maneuverability index of $M = 10$, which gives the ratio $l/b \cong 5$.

Next we focus on the quantity $R = l + b/2$, which represents the spider's *radius*. The choice of R influences the ability of the spider to reach desired footholds along the tunnel walls. To understand this influence, consider a particular triplet of tunnel segments, $I_{i_1}, I_{i_2}, I_{i_3}$. At a 3-legged equilibrium posture the contact-force lines intersect at a common point p. The collection of points p corresponding to all possible equilibrium footholds on $I_{i_1}, I_{i_2}, I_{i_3}$ is a polygonal region denoted P_{i_1,i_2,i_3}. For frictionless contacts P_{i_1,i_2,i_3} is simply the intersection of the strips perpendicular to the segments $I_{i_1}, I_{i_2}, I_{i_3}$. The collection of all polygons P_{i_1,i_2,i_3}, where i_1, i_2, i_3 range over the tunnel segments, describes all possible 3-legged equilibrium postures in a given tunnel.

Next we impose a reachability constraint on the polygons P_{i_1,i_2,i_3}. Figure 4 shows a randomly selected piecewise-linear tunnel whose average width is one unit. For each triplet $I_{i_1}, I_{i_2}, I_{i_3}$ of tunnel segments, we first determine the corresponding equilibria polygon P_{i_1,i_2,i_3}. Then we discretize P_{i_1,i_2,i_3}, and for each point $p \in P_{i_1,i_2,i_3}$ perform the following two steps. First we determine the location of the footholds corresponding to p on $I_{i_1}, I_{i_2}, I_{i_3}$. Then we plot the region formed by intersecting three discs of radius R (the spider's radius), centered at the three footholds. The resulting *reachability region* represents all central-body locations from which some equilibrium footholds on the segments $I_{i_1}, I_{i_2}, I_{i_3}$ can be reached. Figure 4 shows the resulting reachability regions for several spider diameters. To allow a continuous motion of the central-body, R should be chosen such that the reachability regions form a contiguous area along the tunnel. As the figure shows, a spider diameter of $2R = 1.15$ units already provides ample overlap of the reachability regions. In our experiment the tunnel's average width is 1.1 m, and we selected the spider's diameter as $2R = 1.3$ m. Combining the equations $2R = 2l + b = 1.3$ with $l/b = 5$, the limbs' length is $l = 60$ cm and the central-body's size is $b = 12$ cm.

3.3 Limbs Mechanical Design

First we describe how the limbs are attached to the central body, which is made of a square plate. To minimize inter-link interference, we designed two types of limbs—an upper and a lower limb. In an upper limb all driving mechanisms are positioned upward, above the plane of the central body. In a lower limb all driving mechanisms are positioned downward, underneath the central body. We attached two upper limbs and two lower limbs to the central body. As Figure 5(a) shows, the upper limbs never interfere with the lower limbs. Further, to minimize interference between the upper (lower) limbs, the upper (lower) limbs are attached at diagonally opposite corners of the central-body. The resulting design allows simultaneous motion of the four limbs with little inter-link interference.

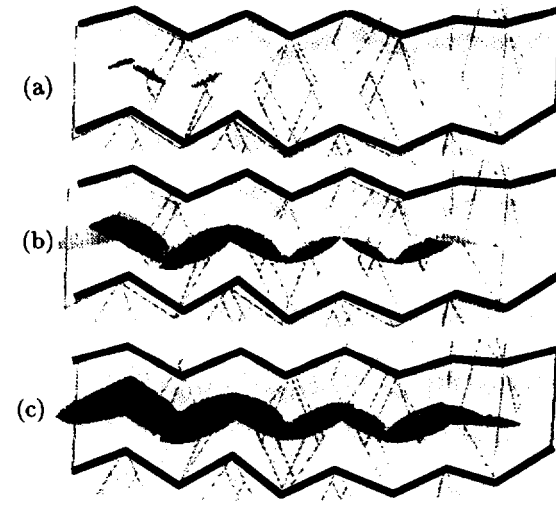

Figure 4. Reachability regions corresponding to a unit-width tunnel. (a) $2R = 0.85$ units, (b) $2R = 1.05$ units, (c) $2R = 1.15$ units. (Courtesy of Eran Guy.)

Finally, to achieve maximum motion flexibility of each limb, we selected the links' length in a *decreasing* order. The link closest to the central-body is 24 cm long, and the next ones have lengths of 18 cm, 14 cm, and 4 cm. These lengths allow each limb to completely retract into the first link, allowing the spider to maneuver itself in congested environments and through narrow passageways. Figure 5(b) shows an upper limb in its retracted configuration.

3.4 Footpad Mechanical Design

The distal links of the limbs are the only parts of the spider that contact the environment, and these links are called *footpads*. Recall that during 3-legged bracing, the footpads' curvature must be sufficiently flat to guarantee immobilization of the spider. Since the tunnel walls are assumed piecewise linear, perfectly flat footpads would give the best immobilization. However, we wish to avoid the overhead incurred by controlling the placement of such footpads. We therefore designed two types of footpads which are easier to control. The first footpad design, shown in Figure 6(a), is a simple rigid-

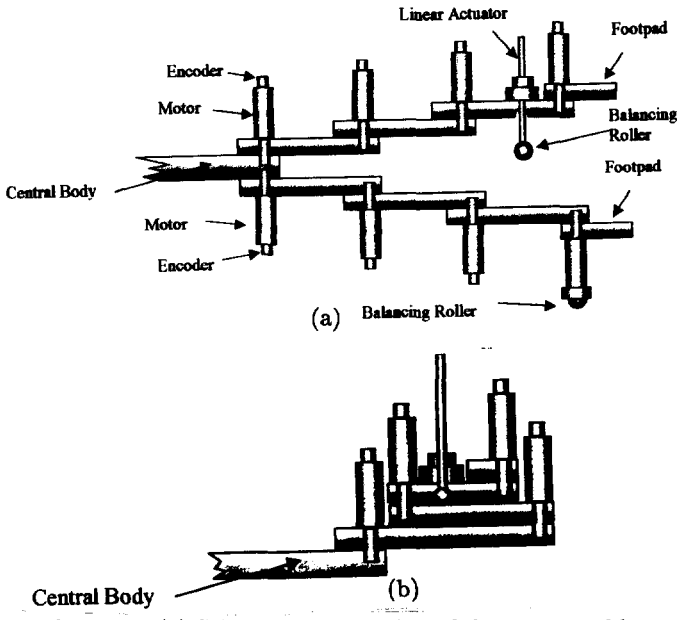

Figure 5. (a) Schematic description of the upper and lower limbs. (b) An upper limb in its retracted configuration.

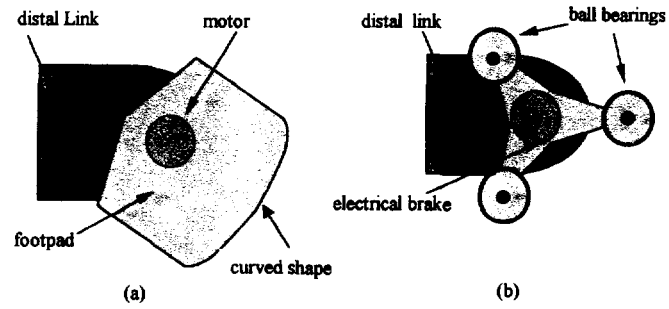

Figure 6. Two footpad designs. (a) A geometric curvature design. (b) A frictionless contact design.

body curved with a large radius-of-curvature that guarantees immobilization. This footpad easily establishes a point-contact with the environment, and by controlling the location of the footpads' contacts we can establish immobile equilibrium postures.

The second footpad design simulates a flat footpad (which gives maximal immobilization), while avoiding the overhead involved in placing a flat footpad on a flat surface. This footpad reduces the contact friction to almost zero, allowing validation of the spider's locomotion in a truly slippery environment. As Figure 6(b) shows, the footpad mechanism consists of a rotating triangular flange with two roller-bearings at each edge, and an electronic clutch that controls the flange's rotation axis. When the footpad reaches a contact surface, the clutch is released and one of the edges passively adjusts itself to the contact surface. When contact is established, the clutch is activated and the footpad becomes a rigid body with two roller-bearings in contact with the environment. The bearings allow only perpendicular forces to be transferred at the contacts, thereby emulating a truly slippery environment.

4 The Spider Robot Motion

We now describe a motion paradigm that allows quasistatic locomotion of the spider in a slippery tunnel environment. The motion consists of two phases which repeat until the spider reaches its goal. In the first phase, called *limb repositioning*, the spider braces itself against the environment with three limbs while the fourth limb moves toward a new foothold. At the end of this phase all four limbs contact the environment. However, before the spider can lift a new limb, it must ensure that the remaining three limbs form an equilibrium posture. For clarity, let the limbs be denoted L_1, L_2, L_3, L_4. Suppose that the spider initially lifts the limb L_1, while the limbs L_2, L_3, L_4 maintain a 3-legged equilibrium posture (Figure 7(a)). To be able to lift a new limb, say L_4, the spider must first ensure that the force-lines of the limbs, L_1, L_2, L_3 intersect at a common point. However, the limbs L_2, L_3 are common to both limb-triplets, and their force-lines intersect at a unique point. Hence we must first move the location of the contact points of the limbs L_2, L_3 before L_4 can be lifted.

In the second phase, called *central-body repositioning*, the spider slides two limbs along the tunnel walls while maintaining a fixed contact with the other two limbs. Using the notation introduced above, the spider slides the limbs L_2, L_3 along the tunnel walls, while the limbs L_1, L_4 maintain a fixed contact with the environment (Figure 7(b)). During this sliding, the intersection point of the force-lines of L_2 and L_3 moves forward, until it reaches the stationary force-line of L_1. Now the limbs L_1, L_2, L_3 form a 3-legged equilibrium posture, and the spider can lift the limb L_4. Note that in both modes of locomotion the spider is continuously immobile with respect to the tunnel walls. During limb-repositioning the spider is immobilized by surface curvature effects ($m^1_{q_0} > 0$ and $m^2_{q_0} = 0$). During central-body repositioning the spider is immobilized by first-order effects ($m^1_{q_0} = 0$). Immobilization implies that the naturally occurring compliance at the contacts stabilize the mechanism against any external perturbation [15]. Hence, if the inertial forces due to moving parts of the spider are kept small, the reaction forces at the contacts would automatically compensate for the inertial forces, resulting in a *locally stable locomotion*. Other important topics, such as the spider's motion planning and control algorithms, will be described in a future paper.

5 Concluding Discussion

We described a design of a 4-legged spider robot capable of quasistatic locomotion in two-dimensional tunnels.

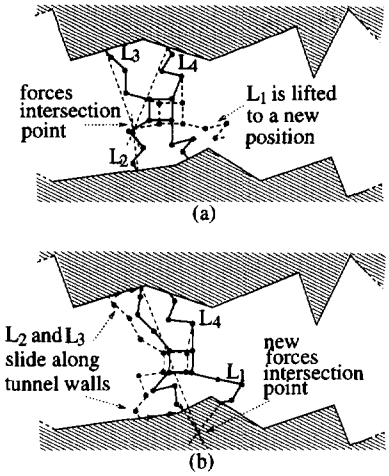

Figure 7. The two motion phases of the spider.

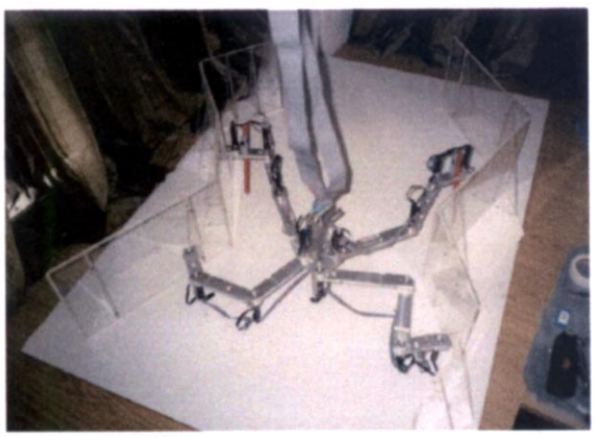

Figure 8. A snapshot showing the spider bracing against tunnel walls.

An immobilization theory dictated the minimal number of limbs such a spider can have, as well as the curvature the footpads must have to guarantee the spider's stability. Other key parameters, such as the dimension and number of degrees of freedom of each limb, were dictated by the class of tunnel geometries. As the spider will initially move under a worst-case assumption of slippery tunnel walls, we also described a locomotion strategy under this assumption. The spider has been built, and a snapshot of the spider bracing against tunnel walls are shown in Figure 8. The spider is currently undergoing initial locomotion experiments, which validate the control algorithms currently being developed for its various modes of locomotion.

References

[1] J.-D. Boissonnat, O. Devillers, L. Donati, F. P. Preparata. Motion planning for spider robots. *ICRA*, 2321–2326, 1992.

[2] G.S. Chirikjian and J.W. Burdick. Design and experiments with a 30 d.o.f. hyper-redundant robot. *ICRA*, 3:113–117, 1993.

[3] J. Czyzowicz, I. Stojmenovic, J. Urrutia. Immobilizing a polytope. *Lecture Notes in Computer Science*, volume 519, 214–227. 1991.

[4] S. Hirose and O. Kunieda. Generalized standard foot trajectory for a quadruped walking vehicle. *The Int. J. of Robotics Research*, 10(1):2–13, 1991.

[5] S. Hirose and A. Morishima. Design and control of a mobile robot with an articulated body. *The Int. J. of Robotics Research*, 9(2):99–114, 1990.

[6] A. Madhani and S. Dubowsky. Motion planning of mobile multi-limb robotic systems subject to force and friction constraints. *ICRA*, 233–239, 1992.

[7] D. W. Marhefka and D. E. Orin. Gait planning for energy efficiency in walking machines. *ICRA*, 474–480, 1997.

[8] X. Markenscoff, L. Ni and C. H. Papadimitriou. The geometry of grasping. *The Int. J. of Robotics Research*, 9(1):61–74, 1990.

[9] T. McGeer. Powered flights, child's play, silly wheels and walking machines. *ICRA*, 1592–1597, 1989.

[10] W. Neubauer. Spider-like robot that climbs vertically in ducts or pipes. *IEEE/RSJ International Conference on Intelligent Robots and Systems*, 2:1178–1185, 1994.

[11] F. Pfeiffer, J. Eltze, H.-J. Weidemann. Six-legged walking considering biological principals. *Robotics and Autonomous Systems*, 223–232, 1995.

[12] F. Reuleaux. *The Kinematics of Machinery*. Macmillan 1876, republished by Dover, NY, 1963.

[13] E. Rimon and J. W. Burdick. A configuration space analysis of bodies in contact—1^{st} order mobility and 2^{nd} order mobility. *Mechanisms and Machine Theory*, 30(6):897–928, 1995.

[14] E. Rimon and J. W. Burdick. New bounds on the number of frictionless fingers required to immobilize planar objects. *J. of Robotic Systems*, 12(6):433–451, 1995.

[15] E. Rimon and J. W. Burdick. Mobility of bodies in contact—ii: How forces are generated by curvature effects. *IEEE Trans. on Robotics and Automation*, 14(5):709–717, 1998.

[16] Y. Shan and Y. Koren. Design and motion planning of a mechanical snake. *IEEE Trans. on Systems Man and Cybernetics*, 23(4):1091–1100, 1993.

[17] T. J. Stone, D. S. Cook, B. L. Luk. Robug iii - the design of an 8-legged teleoperated walking and climbing robot for disordered hazardous environments. *Mechanical Incorporated Engineer*, 7(2):37–41, 1995.

[18] K. van der Doel and D. K. Pai. Performance measures for locomotion robots. *J. of Robotic Systems*, 14(2):135–147, 1997.